NASA TN D-212

TECHNICAL NOTE

D-212

AXIAL-LOAD FATIGUE TESTS OF 2024-T3 AND 7075-T6 ALUMINUM-ALLOY SHEET SPECIMENS UNDER CONSTANT- AND VARIABLE-AMPLITUDE LOADS

By Eugene C. Naumann, Herbert F. Hardrath, and David E. Guthrie

Langley Research Center
Langley Field, Va.

NATIONAL AERONAUTICS AND SPACE ADMINISTRATION

WASHINGTON

December 1959

NATIONAL AERONAUTICS AND SPACE ADMINISTRATION

TECHNICAL NOTE D-212

AXIAL-LOAD FATIGUE TESTS OF 2024-T3 AND 7075-T6 ALUMINUM-ALLOY SHEET SPECIMENS UNDER CONSTANT- AND VARIABLE-AMPLITUDE LOADS

By Eugene C. Naumann, Herbert F. Hardrath, and David E. Guthrie

SUMMARY

Sheet specimens of 2024-T3 and 7075-T6 aluminum alloy with a theoretical elastic stress concentration factor $K_T = 4.0$ were subjected to repeated axial loads. The load amplitude was held constant or varied by steps to approximate a gust load history. The variable-amplitude test data were analyzed assuming linear cumulative damage, and a limited statistical analysis was used to confirm conclusions. The value of the summation of cycle ratios $\sum \frac{n}{N}$ was found to vary with material, loading sequence, and mean stress.

In addition, the possible effects of load spectrum, block size, number of stress steps, and S-N curve reliability are discussed.

INTRODUCTION

In recent years fatigue failures have caused catastrophic failures in both commercial and military aircraft and have contributed to high inspection and maintenance costs. In order to reduce the probability of accidents of this nature, aircraft companies have initiated fatigue test programs on various structural components. These fatigue tests are necessary because there is presently no theory or method that can adequately predict the fatigue life of a component subjected to the randomly varying loading encountered in service. Because of time and cost limitations these fatigue tests are necessarily simplified step tests. These step tests, in turn, raise questions regarding the interpretation of the results obtained.

The present investigation was undertaken in order to help answer some of the questions raised concerning the validity of step testing.

The tests were designed to provide systematic data on the effect of varying such parameters as (1) the sequence of load application; (2) the mean stress on the specimen; (3) the number of load cycles applied to traverse the load sequence one time; (4) the number of load steps; and (5) the gust frequency spectrum which was being approximated. In addition, this investigation provides constant- and variable-amplitude fatigue test data which may be used at some later date in developing a theory or theories which may reduce or eventually eliminate the need for component testing.

Constant- and variable-amplitude axial-load fatigue tests were conducted on notched sheet specimens made of either 2024-T3 or 7075-T6 aluminum alloy. The test results were analyzed by using Miner's hypothesis (ref. 1), and a limited statistical analysis was utilized to determine whether varying the parameters gave significant changes in the results.

SYMBOLS

K_T	theoretical elastic stress concentration factor
N	fatigue life, cycles
n	number of cycles applied at a given stress level
S_{alt}	alternating stress, ksi
S_{max}	maximum stress, ksi
S_{mean}	mean stress, ksi
S_u	ultimate tensile strength of specimen, ksi
V_i	discrete gust velocities, fps

SPECIMENS

The specimens for this investigation were made from part of a stock of commercial 0.090-inch-thick 2024-T3 and 7075-T6 aluminum-alloy sheets retained at the Langley Research Center for fatigue tests. The sheet layouts for this fatigue stock are given in figure 1 of reference 2 and

the material properties are given in table V of reference 3. The tensile properties of these materials are given in table I.

The specimens were cut from material blanks that were numbered in the manner described in reference 2. Ten specimen blanks were cut from each material blank and identified by adding a number (1 to 10) to the material blank number. A typical specimen number might be A117N1-6, where A indicates the material (2024-T3), 117 indicates that the specimen was cut from sheet number 117, N1 indicates the position within the sheet from which the material blank was taken, and 6 indicates the position within the material blank from which the specimen blank was taken.

The specimen dimensions are shown in figure 1(a). The rolled surfaces were left as received and the longitudinal edges were machined and notched in both edges to produce a theoretical elastic stress concentration factor K_T of 4.0. This particular configuration was selected because the fatigue behavior has been found to approximate the fatigue behavior of the best current component designs. (See ref. 4.) The notch was formed by drilling a hole to form the notch root and then slotting with a $\frac{3}{32}$-inch milling tool. In order to minimize residual stresses due to machining, a small hole was drilled first and enlarged to the proper radius by using progressively larger drills. For consistency, only sharp drills were used in a drill press with constant automatic feed. Increments in drill diameters were 0.003 inch.

Burrs left in the machining process were removed by holding the specimen lightly against a small cone of 00 grade steel wool rotating at approximately 1,750 rpm. A schematic diagram of the deburring process is shown in figure 1(b). All specimens were inspected and only those free of surface blemishes in and near the notches were tested.

TESTING MACHINES

Ten axial-load fatigue testing machines (hereinafter referred to by numbers 1 to 10) with nominal capacity of ±20,000 pounds were used for this investigation. The basic machine has a beam excited to vibrate near resonance by a rotating eccentric mass driven at 1,800 cpm by an electric motor. The vibrating beam imparts axial forces to the specimen which acts as one of the supports. Mean loads were applied and maintained by adjusting the preload springs. A more detailed description of these machines is given in reference 3.

Machines 6 to 10 were modified (fig. 2) so that high loads which were to be applied for only a few cycles could be applied accurately.

The modification included the following units: (1) an electrically driven hydraulic pump, (2) a four-way solenoid valve, (3) a hydraulic ram, attached to the lower grip with a removable pin, and (4) a semiautomatic control device with adjustable load-limiting switches, preset counters for semiautomatic operation, and a manual control for applying single load cycles.

The modification made it possible to apply accurately (1) a few medium load amplitudes semiautomatically (preset semiautomatic hydraulic system), and (2) single large-amplitude cycles manually (manual hydraulic system), in addition to the normal capabilities as a subresonant system.

The loads on the specimen were monitored by utilizing weigh bars, equipped with strain gages, in series with the specimen. For subresonant loading the strain-gage output was fed into an alternating-current null-bridge circuit the output of which was monitored on an oscilloscope. An additional set of strain gages was added to the weigh bars for use with the semiautomatic control device for the hydraulic system. The same strain-gage circuit used to monitor the subresonant loading was used to record continuously the loads applied hydraulically.

The load-measuring apparatus was calibrated periodically during this investigation. The error in the load-measuring apparatus was thought not to exceed ±12.5 pounds in the range of loads used. The load on the specimen was maintained within ±25 pounds of the desired load for subresonant loading and within ±50 pounds of the desired load for hydraulic loading.

TEST PROCEDURE

Constant-Amplitude Tests

Those specimens which were expected to fail after more than 10,000 cycles had been applied were tested in machines 1 to 5 at 1,800 cpm using the procedure described in reference 3. The modified machines were used hydraulically for those tests which were expected to end before 10,000 cycles had been applied. Both methods of loadings were used to perform a limited number of tests which lasted about 10,000 cycles in order to provide a check on possible speed effects.

Variable-Amplitude Tests

All the variable-amplitude tests (except six tests which were conducted in machine 10) were conducted in the modified machines (6 to 9). For each stress step in these tests the preset counter was set for the desired number of cycles and the load-limiting switches were adjusted to

produce the desired maximum and minimum loads in the specimen. Once properly adjusted, the load application was automatic and required only occasional monitoring. The machine stopped loading automatically when the predetermined number of cycles had been applied. The counter and load-limiting switches were reset manually for the next stress step. All the loading schedules utilized the three capabilities of the modified machine.

Since it is assumed that any machine differences would be eliminated by the calibration method used, no special effort was made to program the order in which the tests were conducted. In general, similar tests were conducted concurrently. However, because of machine failures and unusually long-lived specimens this was not always possible.

Loading schedules.- The loading schedules used in this investigation were calculated to approximate the gust frequency spectra A or B given in reference 5. Gust velocities were converted to stresses on the assumption that stress is directly proportional to gust velocity and that a 30-fps gust produced design limit stress $\left(\frac{2}{3} S_u\right)$. Thus, alternating stress amplitudes were computed by the simple relation

$$S_{alt} = \left(\frac{2}{3} S_u - S_{mean}\right)\frac{V_i}{30}$$

The mean stresses used in these tests were chosen to cover a range of values which might be used in design of aircraft. The highest values were 17.4 ksi for 2024-T3 and 20 ksi for 7075-T6. These maximum values correspond approximately to the stress which is obtained by using a design limit load factor of 2.5 in combination with the static strength of these specimens (for 2024-T3, the specimen static strength is 65.4 ksi and for 7075-T6, it is 79.8 ksi).

The preceding relationship was used to obtain a stress frequency spectrum for each combination of mean stress, material, and gust spectrum used in this investigation. A typical stress frequency spectrum computed in this manner is shown in figure 3. This particular spectrum is for 7075-T6 aluminum-alloy specimens tested with zero mean stress and represents gust frequency curve A from reference 5. This stress frequency spectrum was reduced to an eight-step loading schedule by using a numerical integration process. The stress frequency spectrum was first divided into eight equal stress bands (defined by horizontal dashed lines in fig. 3). An increment of linear cumulative damage $\left(\sum \frac{n_i}{N}\right)$ was computed for each stress band by further subdividing the stress band into 5 to 10 stress increments and computing a value of n_i/N for each increment. The values of N for this computation were taken from the S-N curves

shown in figures 6 and 9 of reference 6 and figure 8 of reference 7 (except for 2024-T3 aluminum alloy with S_{mean} = 17.4 ksi). The number of cycles n_i for each stress increment was taken from the stress frequency spectrum. The sum of the values of n_i equaled the number of cycles in the stress band (vertical solid lines in fig. 3). The stress level to represent that stress band (horizontal solid lines in fig. 3) was then chosen to yield a value of n/N equal to the value of $\sum \frac{n_i}{N}$ computed for the same stress band. Because of the relative slopes of the stress frequency spectrum and the S-N curve at various levels, the representative stress level for each band fell at a different relative position within the band it represented. Toward the low-stress end of the spectrum the stress levels applied in the tests were below the middle of the band by about 10 percent of the band width. Consequently, stress levels for stress bands including stresses for which $N \to \infty$ were chosen by arbitrarily placing them 10 percent below the middle of the band they represent.

The load schedule just described was modified by multiplying all numbers of cycles n by an arbitrary factor so that $\sum \frac{n}{N}$ for one traverse of the schedule, hereinafter called a "block," was approximately 0.1. Thus, according to Miner's hypothesis $\left(\sum \frac{n}{N} = 1, \text{ ref. } 1\right)$, failure would be expected when 10 blocks have been applied. In some cases the block size was arbitrarily modified in order to investigate the effect of this parameter on the results.

All the eight-step schedules were prepared in the above manner. In addition, 18-step schedules were prepared by dividing the stress frequency spectrum into 18 equal stress bands and representing each stress band by the median stress in that stress band.

Schedules were prepared for each of the following conditions:

2024-T3			7075-T6		
S_{mean}, ksi	Stress steps	Gust frequency spectrum	S_{mean}, ksi	Stress steps	Gust frequency spectrum
17.4	18	B	20	8	A
17.4	18	A	10	8	A
17.4	8	A	0	8	A
0	8	A			

The values of stress, cycles, and n/N for each stress step for each of these conditions are given in tables II and III.

Loading sequence.- The loading sequence refers to the order in which the stress steps were applied in each block. The sequences used were as follows:

(1) Lo-Hi: Lo-Hi sequences started with the lowest stress step and proceeded through successively higher stress steps to the highest stress step. (See fig. 4(a).)

(2) Hi-Lo: Hi-Lo sequences started with the highest stress step and proceeded through successively lower stress steps to the lowest stress step. (See fig. 4(b).)

(3) Lo-Hi-Lo: Lo-Hi-Lo sequences started (with one-half the number of cycles normally applied at each stress step) with the lowest stress step, proceeded through successively higher stress steps to the highest stress step, and then proceeded through successively lower stress steps to the lowest stress step. (See fig. 4(c).)

(4) Hi-Lo-Hi: Hi-Lo-Hi sequences started (with one-half the number of cycles normally applied at each stress step) with the highest stress step, proceeded through successively lower stress steps to the lowest stress step, and then proceeded through successively higher stress steps to the highest stress step. (See fig. 4(d).)

(5) Random: Random sequences started with an arbitrarily chosen stress step and proceeded through the remaining stress steps according to a schedule taken from a table of random numbers. A different stress-step sequence was used for each of the first 20 blocks (hereinafter called random blocks); therefore, a given random sequence was not repeated unless the specimen life exceeded 20 random blocks. (See fig. 4(e).)

RESULTS

Test Data

Constant-amplitude tests.- The results of the constant-amplitude fatigue tests are given in tables IV and V. These data as well as similar data from references 6 and 7 are shown plotted in figures 5 and 6. In these figures the ticks represent the scatter limits for the combined data, the symbols represent the geometric means of the fatigue lives at a given stress level, and the number corresponds to the number of data points represented by the geometric mean. The solid curves represent S-N curves faired through the data.

Variable-amplitude tests.- The results of the variable-amplitude fatigue tests are presented in tables VI and VII. The tests are divided into groups which are defined by six parameters. These parameters are: (1) material, (2) mean stress, (3) gust frequency spectrum approximated, (4) number of load steps, (5) load sequence, and (6) number of cycles per block.

Included in the tables is the number of the machine in which the specimen was tested, the block and load step at failure, and the specimen life (total cycles).

Analysis of Data

Because there were six different parameters to be evaluated in this investigation a common denominator was necessary in order to compare the different groups of variable-amplitude test data. The linear cumulative damage index $\sum \frac{n}{N}$ was selected as the basis of comparison because of its simplicity and generally accepted usage. Therefore, all the variable-amplitude test results were reduced to a value of $\sum \frac{n}{N}$. The values of N were taken from the S-N curves in figures 5 and 6.

When all the test data in each group had been reduced to a value of $\sum \frac{n}{N}$, the Proschan method[1] was used to eliminate any test in which the $\sum \frac{n}{N}$ value was widely displaced from the $\sum \frac{n}{N}$ values of the other tests in that group. This method eliminated only 4 tests of 118, which are identified in tables VI and VII by footnotes. The same method was used to test constant-amplitude data and only 1 point was discarded.

The values of $\sum \frac{n}{N}$ for the variable-amplitude tests are given in tables VI and VII. In addition, the values of $\sum \frac{n}{N}$ are presented graphically in figures 7 and 8. In figures 7 and 8 the ticks represent the scatter in the test data, the symbols represent the geometric mean of the group of data, and the number corresponds to the number of tests in that group.

In order to establish more definitely whether an effect was present the data were compared statistically, with reference 8 as a guide. Two groups of tests differing in only one variable were used for each comparison. In order to make this statistical analysis the distribution of $\sum \frac{n}{N}$ was assumed to be log normal and a 95-percent confidence level was used.

[1]Unpublished paper: "How to Decide Objectively Whether an Outlying Observation Should be Rejected," by Frank Proschan, 1952.

The standard deviations of the logarithms of $\sum \frac{n}{N}$ were compared by the "F" test (i.e., sample standard deviations are (or are not) significantly different) and the means of the logarithms of $\sum \frac{n}{N}$ were compared by the "t" test (i.e., sample means are (or are not) significantly different).

The results of the "t" tests and the ratio of the geometric means for each of the test groups compared are presented in table VIII.

DISCUSSION OF RESULTS

General

The scatter in the constant-amplitude tests was not considered excessive (ticks in figs. 5 and 6) even when data from the present investigation were combined with data from references 6 and 7. The limited data on effect of speed indicated that this parameter caused no appreciable effect in the range investigated. However, as the present data were added to those obtained in previous investigations, the S-N curves changed shape somewhat. For example, the final shapes of curves for 7075-T6 specimens are compared in figure 9 with the curves presented in references 6 and 7. The significance of this change in fairing is discussed in a later section.

The scatter in the variable-amplitude tests (ticks in figs. 7 and 8) was generally less than in the constant-amplitude tests and seldom exceeded 2 to 1 for any group of test data.

During the early phases of this investigation the variable-amplitude tests conducted in machine 6 consistently had the highest value of $\sum \frac{n}{N}$ for a particular test group; however, the specimens tested in machine 9 produced the highest values in the later phases of the investigation.

In general, the values of $\sum \frac{n}{N}$ obtained from tests on 7075-T6 specimens were higher than those for 2024-T3 specimens (figs. 7 and 8). The value of $\sum \frac{n}{N}$ was found to increase with increasing mean stress and to vary with the sequence in which the loads were applied. In addition, the value of $\sum \frac{n}{N}$ seemed to vary with the number of cycles per block, the number of stress steps, and the gust frequency curve.

Sequence Effect

Among groups of tests differing only in the sequence in which the stresses were applied, the highest values of $\sum \frac{n}{N}$ were obtained in tests conducted with the Hi-Lo sequence and the lowest values were obtained in tests conducted with the Lo-Hi sequence. The Random, Lo-Hi-Lo, and Hi-Lo-Hi sequences resulted in intermediate values of $\sum \frac{n}{N}$ with some tendency for results of Lo-Hi-Lo and Hi-Lo-Hi tests to be higher than the results of tests with the Random sequence. The summary of the statistical analysis presented in table VIII(a) indicates that the foregoing observations were supported in the great majority of cases. For example, the values of $\sum \frac{n}{N}$ for the tests with Lo-Hi sequence are shown to be significantly lower than those for other sequences in all cases where comparisons were possible. Similarly, the values of $\sum \frac{n}{N}$ for tests with the Hi-Lo sequence were significantly higher than others in all but two cases. Differences between $\sum \frac{n}{N}$ for Random sequence and for Hi-Lo-Hi or Lo-Hi-Lo were smaller and significant in only two of seven possible cases.

If the random sequence may be regarded as being most nearly representative of service experience, it would appear that considerable bias was introduced in the tests with Lo-Hi and Hi-Lo sequences of loading. Additional work is needed to determine which of the sequences used in this investigation reproduces service loadings most faithfully.

One possible explanation for high values of life in Hi-Lo sequence tests is that beneficial residual compressive stresses were produced by application of high tensile loadings early in the test.

Effect of Mean Stress

Values of $\sum \frac{n}{N}$ were consistently higher for tests with high values of mean stress than for tests with lower values. This observation is supported strongly by the statistical analysis (table VIII(b)) in all cases where comparisons were possible between tests with 0 and 17.4 ksi for 2024-T3 and between tests with 0 and 20 ksi mean stress for 7075-T6. Differences between results of tests with mean stresses of 0 and 10 ksi were not statistically significant.

The probable reason for this behavior is that beneficial residual stresses produced by tensile loadings are effective when the mean stress

is positive, but are canceled by compression loads when the mean stress is zero (ref. 9). The tests with S_{mean} = 10 ksi are probably marginal as regards their ability to show an effect.

Material

Values of $\sum \frac{n}{N}$ computed for results of tests of 7075-T6 specimens were consistently higher than those for corresponding tests of 2024-T3 specimens; the statistical analysis indicated that these differences were significant in all but two cases. (See table VIII(c).) This conclusion is probably less significant than is indicated by the statistical analysis because the calculations of $\sum \frac{n}{N}$ are based upon S-N curves for two different materials.

Number of Cycles Per Block

Comparisons to evaluate the effect of block size on $\sum \frac{n}{N}$ are possible in only six cases (table VIII(d)). The results of these comparisons are quite inconsistent. In three of the six cases the statistical treatment indicated that smaller blocks produced significantly higher values of $\sum \frac{n}{N}$ than did larger blocks; in the other three cases the effects were not significantly different. It should be pointed out that block sizes in the present investigation were varied within a limited range. It is possible that effects would be found if much larger blocks were used. Considerably more data would be required to establish whether variations in block size in a practical range produce a significant effect on specimen life.

Number of Stress Steps

The data are not sufficient to evaluate the effect of the number of stress steps used to simulate the stress spectrum. Table VIII(e) presents conflicting data on this point.

Shape of Stress Frequency Spectrum

The data are insufficient to allow critical evaluation of the shape of the stress frequency spectrum. The one comparison shown in table VIII(f) is inconclusive; this is not surprising since other data (ref. 10) indicate

no consistent effect even for spectra which differ much more than the spectra used in the present investigation.

S-N Curve Reliability

As noted previously, the S-N curves were refaired as indicated in figure 9 after additional constant-amplitude test results were obtained in the present investigation. Since the value of fatigue life N is taken from the S-N curve the cycle ratios, n/N, were greatly affected by this revision in the S-N curves. In some cases individual stress band cycle ratios changed more than 100 percent and the sum of the cycle ratios $\sum \frac{n}{N}$ for the load schedule as much as 35 percent. The results presented in tables VI and VII and figures 7 and 8 were obtained using the revised S-N curves, but the S-N curves taken from references 6 and 7 were used in the numerical-integration process for determining the test schedules. It was found that by using the revised S-N curves the numerical integration would have yielded different values of stresses to represent the stress bands in some cases. The preceding discussion clearly shows the necessity for establishing a representative S-N curve, particularly if the values of $\sum \frac{n}{N}$ obtained from tests on similar specimen configurations are to be used for comparative purposes. Failure to establish a reasonably reliable S-N curve may be responsible for some of the large variations in $\sum \frac{n}{N}$ or other life index used in discussing results of variable-amplitude fatigue tests in the literature.

L 7 9 8

Stress at Failure

For 7075-T6 specimens the stress step in which specimen failure occurred had a definite pattern. For S_{mean} = 0 ksi most of the specimens failed at the higher stresses while for S_{mean} = 20 ksi most of the specimens failed at the lower stresses. (See fig. 10.) The pattern was not so clear for 2024-T3 specimens; however, fewer tests with eight steps were made. The sequence in which the loads were applied did not seem to affect the load at failure.

CONCLUSIONS

The results of programmed variable-amplitude axial-load fatigue tests of 2024-T3 and 7075-T6 aluminum-alloy sheet specimens support the following conclusions:

1. The values of the summation of cycle ratios $\sum \frac{n}{N}$ for 7075-T6 specimens were consistently higher than the values obtained for 2024-T3 specimens.

2. The sequence in which the loads are applied has a marked effect on the life of the specimen, with sequences involving progressively increasing stresses within each block giving the shortest life and sequences involving progressively decreasing stresses in each block giving the longest life.

3. The mean stress at which the specimen is tested has an effect on $\sum \frac{n}{N}$, with the life increasing as the mean stress is increased.

4. A reasonable change in the fairing of the S-N curve produces an appreciable change in the value of $\sum \frac{n}{N}$.

5. Additional data are needed to establish effects due to the number of load cycles per block, the number of load steps used to approximate the load spectrum, and changes in the load spectrum.

Langley Research Center,
National Aeronautics and Space Administration,
Langley Field, Va., October 6, 1959.

REFERENCES

1. Miner, Milton A.: Cumulative Damage in Fatigue. Jour. Appl. Mech., vol. 12, no. 3, Sept. 1945, pp. A-159 - A-164.

2. Grover, H. J., Bishop, S. M., and Jackson, L. R.: Fatigue Strengths of Aircraft Materials. Axial-Load Fatigue Tests on Unnotched Sheet Specimens of 24S-T3 and 75S-T6 Aluminum Alloys and of SAE 4130 Steel. NACA TN 2324, 1951.

3. Grover, H. J., Hyler, W. S., Kuhn, Paul, Landers, Charles B., and Howell, F. M.: Axial-Load Fatigue Properties of 24S-T and 75S-T Aluminum Alloy as Determined in Several Laboratories. NACA Rep. 1190, 1954. (Supersedes NACA TN 2928.)

4. Spaulding, E. H.: Design for Fatigue. SAE Trans., vol. 62, 1954, pp. 104-116.

5. Rhode, Richard V., and Donely, Philip: Frequency of Occurrence of Atmospheric Gusts and of Related Loads on Airplane Structures. NACA WR L-121, 1944. (Formerly NACA ARR L4I21.)

6. Illg, Walter: Fatigue Tests on Notched and Unnotched Sheet Specimens of 2024-T3 and 7075-T6 Aluminum Alloys and of SAE 4130 Steel With Special Consideration of the Life Range From 2 to 10,000 Cycles. NACA TN 3866, 1956.

7. Grover, H. J., Bishop, S. M., and Jackson, L. R.: Fatigue Strengths of Aircraft Materials. Axial-Load Fatigue Tests on Notched Sheet Specimens of 24S-T3 and 75S-T6 Aluminum Alloys and of SAE 4130 Steel With Stress-Concentration Factors of 2.0 and 4.0. NACA TN 2389, 1951.

8. Anon.: A Tentative Guide for Fatigue Testing and the Statistical Analysis of Fatigue Data. Special Tech. Pub. No. 91-A, ASTM, 1958.

9. Anon.: Discussion in New York by Herbert F. Hardrath (Langley Field, Va.). Proc. Int. Conf. on Fatigue of Metals (London and New York), Inst. Mech. Eng. and A.S.M.E., 1956, p. 830.

10. Hardrath, Herbert F., Utley, Elmer C., and Guthrie, David E.: Rotating-Beam Fatigue Tests of Notched and Unnotched 7075-T6 Aluminum-Alloy Specimens Under Stresses of Constant and Varying Amplitudes. NASA TN D-210, 1959.

TABLE I.- TENSILE PROPERTIES OF ALUMINUM-ALLOY MATERIALS TESTED

	Av.	Min.	Max.
7075-T6 (152 tests):			
Yield stress (0.2 percent offset), ksi	75.50	71.54	79.79
Ultimate tensile strength, ksi	82.94	79.84	84.54
Total elongation (2-inch gage length), percent	12.3	7.0	15.0
2024-T3 (147 tests):			
Yield stress (0.2 percent offset), ksi	52.05	46.88	59.28
Ultimate tensile strength, ksi	72.14	70.27	73.44
Total elongation (2-inch gage length), percent	21.6	15.0	25.0

TABLE II.- VARIABLE-AMPLITUDE LOADING SCHEDULES FOR 2024-T3 ALUMINUM-ALLOY SPECIMENS

Step	S_{max}, ksi	n	n/N, per step
S_{mean} = 17.4 ksi; gust frequency curve B			
1	18.1	62,000	0
2	19.5	24,000	0
3	20.9	9,400	.000235
4	22.3	3,400	.002618
5	23.7	880	.003260
6	25.1	220	.002296
7	26.5	60	.001350
8	27.9	26	.001000
9	29.3	7.8	.000520
10	30.7	3.2	.000348
11	32.1	1.8	.000295
12	33.5	.5	.000119
13	34.9	.34	.000117
14	36.3	.16	.000070
15	37.7	.08	.000052
16	39.1	.054	.000047
17	40.5	.024	.000025
18	41.9	.012	.000015
		$\sum$[a]100,000	$\sum$0.012367
S_{mean} = 17.4 ksi; gust frequency curve A			
1	19.5	82,000	0
2	22.5	15,000	.016660
3	25.6	2,800	.038360
4	28.7	350	.018940
5	31.9	46	.007080
6	35.1	7.4	.002680
7	38.4	1.6	.001208
8	41.5	.35	.000466
		$\sum$[b]100,205	$\sum$0.085394

Step	S_{max}, ksi	n	n/N, per step
S_{mean} = 17.4 ksi; gust frequency curve A			
1	18.1	46,800	0
2	19.5	27,200	0
3	20.9	14,500	.000363
4	22.3	6,800	.005230
5	23.7	2,750	.010160
6	25.1	1,120	.011680
7	26.5	490	.010650
8	27.9	200	.007700
9	29.3	80	.005330
10	30.7	39	.004240
11	32.1	18	.002918
12	33.5	7.6	.001810
13	34.9	3.0	.001035
14	36.3	1.3	.000634
15	37.7	.6	.000387
16	39.1	.3	.000261
17	40.5	.25	.000153
18	41.9	.09	.000113
		$\sum$100,000	$\sum$0.062664
S_{mean} = 0; gust frequency curve A			
1	2.2	41,000	0
2	8.0	7,850	.001869
3	13.2	980	.019600
4	18.5	143	.014300
5	23.8	23	.012105
6	29.2	3	.008824
7	34.8	.73	.004294
8	40.4	.11	.001896
		$\sum$[c]50,000	$\sum$0.062888

[a]Tests were also made at 5n.
[b]Tests were also made at n/2.
[c]Tests were also made at 2n.

TABLE III.- VARIABLE-AMPLITUDE LOADING SCHEDULES

FOR 7075-T6 ALUMINUM-ALLOY SPECIMENS

Step	S_{max}, ksi	n	n/N, per step
S_{mean} = 20 ksi; gust frequency curve A			
1	21.5	42,000	0
2	25.3	7,500	.046875
3	28.7	1,190	.071687
4	32.6	175	.030172
5	36.3	23	.007931
6	40.1	2.5	.001678
7	43.9	.5	.000610
8	47.5	.1	.000208
		$\sum$[a]50,900	$\sum$0.159161
S_{mean} = 10 ksi; gust frequency curve A			
1	13	24,400	0
2	17.1	4,700	.009038
3	21.9	1,000	.050000
4	27.1	92	.020909
5	31.7	14	.008485
6	36.8	1.8	.002687
7	42.5	.3	.000231
8	47.0	.07	.000121
		$\sum$30,200	$\sum$0.091471
S_{mean} = 0; gust frequency curve A			
1	3.8	24,400	0
2	9.1	4,800	.002087
3	15.0	690	.025091
4	21.2	98	.023333
5	27.2	14	.007778
6	33.7	1.8	.005625
7	39.9	.33	.002538
8	46.3	.074	.001276
		$\sum$30,000	$\sum$0.067728

[a]Tests were also made at n/5.

TABLE IV.- RESULTS OF CONSTANT-AMPLITUDE AXIAL-LOAD FATIGUE TESTS OF 2024-T3 ALUMINUM-ALLOY SPECIMENS WITH K_T = 4.0 EDGE NOTCH

Specimen	S_{max}, ksi	Life, cycles	Specimen	S_{max}, ksi	Life, cycles
S_{mean} = 0 ksi					
A36N2-2	34.5	174	A29N2-5	10	716,000
A26N2-5	34.5	146	A29N2-9	10	300,000
			A29N2-6	10	197,000
A29N2-1	18	15,000			
A29N2-2	18	14,000	A26N2-7	8	6,284,000
A29N2-8	18	13,000	A27N2-6	8	4,609,000
A29N2-3	18	12,000	A27N2-7	8	4,488,000
A29N2-4	18	8,000	A27N2-8	8	3,663,000
			A26N2-6	8	3,361,000
A26N2-1	12	233,000			
A29N2-10	12	211,000	A36N2-1	7.25	5,318,000
A27N2-5	12	178,000			
A26N2-4	12	126,000	A27N2-10	7	17,039,000
A29N2-7	12	113,000	A36N2-4	7	4,148,000
S_{mean} = 17.4 ksi					
A39S1-10	44	572	A42S1-2	27.5	73,000
A43S1-3	44	557	A42S1-6	27.5	71,000
A42S1-7	44	534	A38S1-6	27.5	29,000
A39S1-2	44	529	A42S1-4	27.5	26,000
A43S1-6	44	475	A42S1-5	27.5	23,000
A39S1-6	42	825	A47S1-6	25	64,000
			A47S1-5	25	62,000
A39S1-4	40	1,157	A48S1-2	25	58,000
A39S1-7	40	1,059	A48S1-8	25	57,000
A39S1-1	40	797	A48S1-10	25	49,000
A43S1-8	40	793			
A44S1-6	40	722	A41S1-7	22.5	4,810,000
A42S1-1	40	762	A41S1-3	22.5	346,000
			A41S1-10	22.5	274,000
A44S1-7	38	1,470	A41S1-8	22.5	231,000
			A46S1-7	22.5	155,000
A39S1-3	36	3,252			
A44S1-10	36	2,442	A46S1-5	22	47,106,000
A39S1-5	36	1,897	A41S1-5	22	23,343,000
A43S1-4	36	1,691	A47S1-9	22	16,479,000
A43S1-9	36	1,380	A41S1-9	22	10,204,000
			A38S1-1	22	9,817,000
A40S1-3	34	3,568	A38S1-2	22	6,167,000
			A41S1-4	22	5,496,000
A39S1-8	32	15,893	A37S1-10	22	551,000
A43S1-10	32	12,473	A38S1-9	22	255,000
A40S1-8	32	9,833	A48S1-6	22	214,000
A39S1-9	32	6,641			
A43S1-5	32	5,544	A37S1-7	21	>169,709,000
			A37S1-9	21	146,780,000
A47S1-1	30	14,000	A37S1-3	21	141,040,000
A47S1-10	30	14,000	A37S1-8	21	>112,905,000
A46S1-6	30	13,000	A45S1-8	21	>110,430,000
A46S1-10	30	12,000	A45S1-6	21	>70,568,000
A47S1-7	30	11,000	A37S1-4	21	53,157,000
			A37S1-1	21	52,381,000
			A45S1-3	21	14,952,000
			A46S1-2	21	605,000

TABLE V.- RESULTS OF CONSTANT-AMPLITUDE AXIAL-LOAD FATIGUE TESTS OF 7075-T6 ALUMINUM-ALLOY SPECIMENS WITH K_T = 4.0 EDGE NOTCH

Specimen	S_{max}, ksi	Life, cycles	Specimen	S_{max}, ksi	Life, cycles
S_{mean} = 0 ksi					
B55N1-5	50	40	B55N1-6	12	149,000
B55N1-4	50	36	B60N1-7	12	130,000
			B88N1-1	12	95,000
B59N1-10	40	136			
B59N1-9	40	130	B59N1-6	10	1,292,000
			B59N1-2	10	673,000
B60N1-4	30	917	B59N1-5	10	532,000
B60N1-2	30	863	B59N1-4	10	456,000
B129S1-8	30	654	B59N1-3	10	310,000
B59N1-8	20	6,000	B88N1-10	9	3,874,000
B60N1-5	20	6,000	B88N1-7	9	3,309,000
			B88N1-9	9	2,290,000
B60N1-1	15	35,000			
B55N1-1	15	30,000			
B60N1-3	15	18,000			
S_{mean} = 10 ksi					
B88N1-2	50	113	B60N1-9	18	1,106,000
B29N1-4	50	92	B59N1-7	18	162,000
B88N1-4	50	84	B60N1-10	18	52,000
			B60N1-6	18	45,000
B27N1-6	40	440	B60N1-8	18	42,000
B27N1-7	40	374			
			B57N1-2	17	2,241,000
B27N1-2	38.2	453	B57N1-3	17	2,102,000
			B57N1-9	17	1,093,000
B27N1-10	35	955			
			B55N1-10	16	24,204,000
B27N1-9	25	6,823	B88N1-6	16	13,877,000
			B55N1-2	16	8,247,000
B55N1-9	20	57,820			
B27N1-8	20	32,990	B27N1-5	15	>10,000,000
B55N1-3	20	29,000			
B88N1-3	20	22,520			
S_{mean} = 20 ksi					
B55N1-7	50	363	B129S1-4	25	81,000
B55N1-8	50	309	B129S1-7	25	75,000
			B128S1-1	25	63,000
B57N1-1	30	13,000	B56N1-9	25	42,000
B57N1-10	30	10,800			
B88N1-5	30	9,000	B58N1-9	24.5	9,648,000
			B58N1-10	24.5	5,875,000
B129S1-6	25	674,000	B57N1-5	24.5	176,000
B56N1-8	25	335,000			
B129S1-9	25	120,000	B57N1-8	24	44,606,000
B129S1-10	25	112,000	B57N1-7	24	18,575,000
B129S1-5	25	92,000	B57N1-4	24	8,355,000

TABLE VI.- RESULTS OF VARIABLE-AMPLITUDE AXIAL-LOAD FATIGUE TESTS

OF 2024-T3 ALUMINUM-ALLOY SPECIMENS

(a) S_{mean} = 17.4 ksi; gust frequency curve B; 18 stress steps

Number of cycles per block (approx.)	Specimen	Machine number	Failure		Life, cycles	$\sum \frac{n}{N}$
			Block	Step		
Lo-Hi sequence						
100,000	A115N1-9	6	81	11	8,099,990	0.99
	A116N1-2	8	80	12	7,999,990	.98
	[a]A108N1-3	8	47	12	[a]4,700,470	[a].57
	Geometric mean				8,049,000	0.99
500,000	[a]A48S1-9	10	15	11	[a]7,499,990	[a]0.92
	A36S1-2	10	10	13	5,000,000	.61
	A107N1-1	6	9	8	4,499,810	.54
	A43S1-2	10	9	5	4,773,270	.52
	A47S1-2	10	9	3	4,453,000	.49
	A48S1-4	10	7	12	3,500,000	.43
	A45S1-5	10	7	7	3,499,590	.41
	A102N1-1	7	7	6	3,498,530	.40
	A105N1-1	8	7	3	3,443,700	.37
	A38S1-7	10	5	15	2,500,000	.31
	Geometric mean				3,872,000	0.45
Hi-Lo sequence						
100,000	A107N1-3	6	178	14	17,699,820	2.17
	A107N1-5	7	126	4	12,504,190	1.54
	A115N1-8	7	75	3	7,410,430	.92
	Geometric mean				11,888,000	1.46
500,000	A103N1-1	6	53	5	26,036,740	3.26
	A106N1-3	8	36	4	17,630,560	2.18
	A106N1-5	7	35	3	17,061,470	2.16
	A106N1-1	7	27	3	13,028,160	1.68
	A101N1-1	8	23	5	11,005,980	1.42
	A106N1-4	6	18	4	8,505,990	1.10
	Geometric mean				14,555,000	1.85
Random						
500,000	[a]A110N1-1	6	35	14	[a]17,511,900	[a]2.14
	A109N1-2	7	21	2	10,142,960	1.29
	A101N1-10	8	19	17	9,184,510	1.13
	A109N1-3	7	16	6	7,879,080	1.03
	A105N1-7	8	15	12	7,434,870	.90
	A103N1-9	8	15	6	7,361,740	.89
	A109N1-9	7	15	3	7,060,600	.91
	A110N1-3	8	11	14	5,500,000	.67
	A101N1-7	8	7	4	3,654,000	.38
	Geometric mean				6,988,000	0.85

(b) S_{mean} = 17.4 ksi; gust frequency curve A; 18 stress steps

Number of cycles per block (approx.)	Specimen	Machine number	Failure		Life, cycles	$\sum \frac{n}{N}$
			Block	Step		
Random						
100,000	A119N1-10	8	26	18	2,501,000	1.63
	A120N1-8	7	21	14	2,020,800	1.30
	A105N1-8	7	16	18	1,525,280	.95
	A122N1-7	9	15	17	1,402,930	.90
	Geometric mean				1,824,000	1.16

[a]Not included in geometric mean.

TABLE VI.- RESULTS OF VARIABLE-AMPLITUDE AXIAL-LOAD FATIGUE TESTS

OF 2024-T3 ALUMINUM-ALLOY SPECIMENS - Concluded

(c) S_{mean} = 17.4 ksi; gust frequency curve A; 8 stress steps

Number of cycles per block (approx.)	Specimen	Machine number	Failure		Life, cycles	$\sum \frac{n}{N}$
			Block (b)	Step		
Lo-Hi sequence						
100,200	A116N1-6	7	7	4	701,040	0.57
	A116N1-5	6	6	4	600,890	.48
	A116N1-1	7	5	7	501,110	.43
	Geometric mean				595,400	0.49
Hi-Lo sequence						
100,200	A118N1-7	9	27	2	2,608,550	2.72
	A118N1-8	6	24	5	2,304,790	2.36
	A119N1-7	7	21	2	2,007,310	2.11
	Geometric mean				2,294,000	2.38
Lo-Hi-Lo sequence						
100,200	A115N1-1	7	19D	3	1,853,600	1.61
	A116N1-8	8	16A	7	1,553,190	1.32
	A111N1-5	6	15D	8	1,453,650	1.24
	Geometric mean				1,612,000	1.38
Hi-Lo-Hi sequence						
100,200	A111N1-3	6	18A	2	1,755,830	1.49
	A111N1-2	7	15A	3	1,450,290	1.26
	A111N1-4	6	14A	3	1,375,670	1.16
	Geometric mean				1,518,800	1.30
Random						
50,100	A115N1-3	7	47	6	2,357,950	2.01
	A115N1-4	6	42	7	2,055,210	1.75
	A113N1-4	7	34	6	1,703,500	1.45
	Geometric mean				2,020,000	1.72
100,200	A111N1-6	8	15	7	1,402,940	1.20
	A111N1-1	9	14	5	1,402,840	1.19
	A111N1-7	8	13	7	1,202,470	1.03
	A115N1-2	9	10	3	903,240	.72
	Geometric mean				1,215,000	1.02

(d) S_{mean} = 0 ksi; gust frequency curve A; 8 stress steps

Number of cycles per block (approx.)	Specimen	Machine number	Failure		Life, cycles	$\sum \frac{n}{N}$
			Block	Step		
Random						
50,000	A120N1-7	9	15	8	742,000	0.93
	A121N1-4	9	12	7	551,120	.73
	A121N1-3	8	10	7	458,990	.61
	A117N1-4	8	10	7	458,990	.61
	A122N1-9	9	8	5	399,990	.49
	A120N1-9	9	8	6	349,580	.47
	Geometric mean				478,600	0.62
100,000	A118N1-1	8	4	8	399,670	0.44
	A117N1-9	8	4	8	399,670	.44
	A117N1-5	9	3	5	301,990	.30
	Geometric mean				363,600	0.39

[b] A or D indicates ascending or descending portion of block.

TABLE VII.- RESULTS OF VARIABLE-AMPLITUDE AXIAL-LOAD FATIGUE TESTS

OF 7075-T6 ALUMINUM-ALLOY SPECIMENS

(a) S_{mean} = 20 ksi; gust frequency curve A; 8 stress steps

Number of cycles per block (approx.)	Specimen	Machine number	Failure		Life, cycles	$\sum \frac{n}{N}$
			Block (a)	Step		
Lo-Hi sequence						
10,200	B28N1-9	6	57	4	580,670	1.81
	B33N1-7	8	39	6	396,950	1.24
	B29N1-5	7	37	4	376,550	1.17
	Geometric mean				442,800	1.38
50,900	B31N1-9	6	11	3	558,410	1.64
	B26N1-2	7	10	2	507,520	1.48
	B29N1-2	8	8	3	407,100	1.27
	B29N1-3	8	7	7	356,240	1.12
	Geometric mean				452,400	1.36
Hi-Lo sequence						
50,900	B37N1-4	6	31	6	1,526,730	4.78
	B26N1-5	8	26	2	1,281,170	4.14
	B30N1-5	7	24	1	1,179,380	3.83
	B43N1-8	9	23	2	1,121,300	3.63
	Geometric mean				1,268,000	4.04
Lo-Hi-Lo sequence						
10,200	B33N1-10	6	100D	7	1,012,900	3.17
	B32N1-1	6	93A	4	950,460	2.94
	B33N1-9	8	69A	2	695,820	2.16
	B33N1-8	9	50D	5	508,860	1.59
	Geometric mean				762,000	2.38
Hi-Lo-Hi sequence						
50,900	B58N1-4	6	21A	5	1,068,710	3.38
	B50N1-7	7	21A	4	1,068,700	3.36
	B58N1-7	6	19D	6	916,550	2.87
	B58N1-8	7	18D	7	865,630	2.71
	Geometric mean				975,700	3.05
Random						
10,200	B33N1-6	7	73	2	736,400	2.30
	B30N1-2	8	65	7	661,490	2.06
	B32N1-4	9	58	5	590,050	1.84
	Geometric mean				661,400	2.06
50,900	B28N1-8	7	14	2	712,450	2.22
	B26N1-1	6	14	5	712,440	2.22
	B43N1-7	8	12	3	558,810	1.75
	B43N1-9	9	10	3	458,020	1.43
	Geometric mean				600,300	1.87

[a] A or D indicates ascending or descending portion of block.

TABLE VII.- RESULTS OF VARIABLE-AMPLITUDE AXIAL-LOAD FATIGUE TESTS

OF 7075-T6 ALUMINUM-ALLOY SPECIMENS - Concluded

(b) S_{mean} = 10 ksi; gust frequency curve A; 8 stress steps

Number of cycles per block (approx.)	Specimen	Machine number	Failure		Life, cycles	$\sum \frac{n}{N}$
			Block (a)	Step		
Lo-Hi sequence						
30,200	B46N1-3	7	16A	6	468,170	1.43
	B39N1-6	9	14D	2	410,030	1.29
	B39N1-7	6	12A	4	297,380	1.06
	Geometric mean				385,000	1.25
Random						
30,200	B41N1-9	8	14	1	400,030	1.20
	B41N1-7	6	11	6	326,500	.93
	B39N1-8	8	10	4	277,630	.91
	B42N1-8	9	10	2	272,880	.89
	B41N1-8	7	9	3	242,750	.81
	B42N1-7	6	7	5	211,440	.64
	Geometric mean				282,400	.88

(c) S_{mean} = 0 ksi; gust frequency curve A; 8 stress steps

Number of cycles per block (approx.)	Specimen	Machine number	Failure		Life, cycles	$\sum \frac{n}{N}$
			Block	Step		
Lo-Hi sequence						
30,000	B40N1-2	9	17	6	509,990	1.09
	B39N1-5	6	11	5	320,740	.74
	B41N1-4	9	7	8	210,020	.47
	B39N1-1	7	7	8	210,020	.47
	B40N1-8	6	7	8	210,020	.47
	B45N1-2	7	6	6	179,920	.40
	Geometric mean				254,600	.57
Hi-Lo sequence						
30,000	B40N1-6	9	21	8	600,080	1.36
	B39N1-10	6	21	8	600,080	1.36
	B39N1-3	7	18	7	510,270	1.15
	B46N1-10	7	15	7	420,060	.95
	B38N1-7	7	14	6	390,060	.89
	[b]B37N1-5	7	7	8	[b]210,000	[b].45
	Geometric mean				496,300	1.12
Lo-Hi-Lo sequence						
30,000	B27N1-3	7	21A	6	615,150	1.37
	B26N1-8	8	17A	7	495,080	1.12
	B27N1-4	8	14A	5	405,060	.90
	Geometric mean				497,700	1.11
Random						
30,000	B44N1-9	9	26	7	775,310	1.73
	B43N1-5	9	18	7	540,110	1.22
	B28N1-6	6	14	7	398,150	.91
	B43N1-1	8	12	7	330,830	.80
	B43N1-6	8	12	7	330,830	.80
	B43N1-3	8	7	8	210,010	.47
	Geometric mean				393,900	.91

[a] A or D indicates ascending or descending portion of block.

[b] Not included in geometric mean.

TABLE VIII.- RESULTS OF STATISTICAL ANALYSIS OF VARIABLE-AMPLITUDE FATIGUE TESTS

ON 2024-T3 AND 7075-T6 ALUMINUM-ALLOY SPECIMENS

[In the test-group designation, the letters A and B indicate gust frequency curve, the numbers 8 and 18 indicate stress step, the numbers 10,200 to 500,000 indicate number of cycles per block, the numbers 0, 10, 17.4, and 20 indicate the mean stress, and the terms Lo-Hi, Hi-Lo, etc. indicate the sequence]

(a) Effect of sequence

Side group		Top group: 2024-18-B-17.4-100,000 Lo-Hi	2024-18-B-17.4-100,000 Hi-Lo	2024-18-B-17.4-500,000 Lo-Hi	2024-18-B-17.4-500,000 Hi-Lo	2024-18-B-17.4-500,000 Random	2024-8-A-17.4-100,200 Lo-Hi	2024-8-A-17.4-100,200 Hi-Lo	2024-8-A-17.4-100,200 Lo-Hi-Lo	2024-8-A-17.4-100,200 Hi-Lo-Hi	2024-8-A-17.4-100,200 Random	7075-8-A-20-10,200 Lo-Hi	7075-8-A-20-10,200 Lo-Hi-Lo	7075-8-A-20-10,200 Random	7075-8-A-20-50,900 Lo-Hi	7075-8-A-20-50,900 Hi-Lo	7075-8-A-20-50,900 Hi-Lo-Hi	7075-8-A-20-50,900 Random	7075-8-A-10-30,200 Lo-Hi-Lo	7075-8-A-10-30,200 Random	7075-8-A-0-30,000 Lo-Hi	7075-8-A-0-30,000 Hi-Lo	7075-8-A-0-30,000 Lo-Hi-Lo	7075-8-A-0-30,000 Random
2024-18-B-17.4-100,000	Lo-Hi		Yes																					
2024-18-B-17.4-100,000	Hi-Lo	0.67																						
2024-18-B-17.4-500,000	Lo-Hi				Yes	Yes																		
2024-18-B-17.4-500,000	Hi-Lo			0.24		Yes																		
2024-18-B-17.4-500,000	Random			0.52	2.16																			
2024-8-A-17.4-100,200	Lo-Hi							Yes	Yes	Yes	Yes													
2024-8-A-17.4-100,200	Hi-Lo						0.21		Yes	Yes	Yes													
2024-8-A-17.4-100,200	Lo-Hi-Lo						0.35	1.73		No	No													
2024-8-A-17.4-100,200	Hi-Lo-Hi						0.38	1.84	1.06		No													
2024-8-A-17.4-100,200	Random						0.48	2.35	1.36	1.28														
7075-8-A-20-10,200	Lo-Hi												Yes	Yes										
7075-8-A-20-10,200	Lo-Hi-Lo											0.58		No										
7075-8-A-20-10,200	Random											0.67	1.15											
7075-8-A-20-50,900	Lo-Hi															Yes	Yes	Yes						
7075-8-A-20-50,900	Hi-Lo														0.34		Yes	Yes						
7075-8-A-20-50,900	Hi-Lo-Hi														0.44	1.32		Yes						
7075-8-A-20-50,900	Random														0.73	2.15	1.64							
7075-8-A-10-30,200	Lo-Hi-Lo																			Yes				
7075-8-A-10-30,200	Random																		1.42					
7075-8-A-0-30,000	Lo-Hi																					Yes	Yes	Yes
7075-8-A-0-30,000	Hi-Lo																				0.51		No	No
7075-8-A-0-30,000	Lo-Hi-Lo																				0.51	1.01		No
7075-8-A-0-30,000	Random																				0.62	1.23	1.22	

Yes — Sample geometric means are significantly different

1.78 — Ratio of sample geometric means, $\frac{\text{Top group}}{\text{Side group}}$

TABLE VIII.- RESULTS OF STATISTICAL ANALYSIS OF VARIABLE-AMPLITUDE FATIGUE TESTS ON 2024-T3 AND 7075-T6 ALUMINUM-ALLOY SPECIMENS - Continued

(b) Effect of mean stress

Side group \ Top group		2024-8-A-Random-50,100 17.4	2024-8-A-Random-100,200 17.4	2024-8-A-Random-50,000 0	2024-8-A-Random-100,000 0	7075-8-A-Lo-Hi-10,200 20	7075-8-A-Lo-Hi-50,900 20	7075-8-A-Lo-Hi-30,000 0	7075-8-A-Hi-Lo-50,900 20	7075-8-A-Hi-Lo-30,000 0	7075-8-A-Lo-Hi-Lo-10,200 20	7075-8-A-Lo-Hi-Lo-30,200 10	7075-8-A-Lo-Hi-Lo-30,000 0	7075-8-A-Random-10,200 20	7075-8-A-Random-50,900 20	7075-8-A-Random-30,200 10	7075-8-A-Random-30,000 0
2024-8-A-Random-50,100	17.4			Yes	Yes												
2024-8-A-Random-100,200	17.4			Yes	Yes												
2024-8-A-Random-50,000	0	2.78	1.6														
2024-8-A-Random-100,000	0	4.44	2.6														
7075-8-A-Lo-Hi-10,200	20							Yes									
7075-8-A-Lo-Hi-50,900	20							Yes									
7075-8-A-Lo-Hi-30,000	0					2.4	2.3										
7075-8-A-Hi-Lo-50,900	20									Yes							
7075-8-A-Hi-Lo-30,000	0							3.59									
7075-8-A-Lo-Hi-Lo-10,200	20											Yes	Yes				
7075-8-A-Lo-Hi-Lo-30,200	10										1.89		No				
7075-8-A-Lo-Hi-Lo-30,000	0										2.13	1.12					
7075-8-A-Random-10,200	20															Yes	Yes
7075-8-A-Random-50,900	20															Yes	Yes
7075-8-A-Random-30,200	10													2.33	2.1		No
7075-8-A-Random-30,000	0													2.25	2.0	0.97	

Yes — Sample geometric means are significantly different

1.78 — Ratio of sample geometric means, $\frac{\text{Top group}}{\text{Side group}}$

TABLE VIII.- RESULTS OF STATISTICAL ANALYSIS OF VARIABLE-AMPLITUDE FATIGUE TESTS ON 2024-T3 AND 7075-T6 ALUMINUM-ALLOY SPECIMENS - Continued

(c) Effect of material

Side group \ Top group		Lo-Hi-8-A-20-10,200 7075	Lo-Hi-8-A-20-50,900 7075	Lo-Hi-8-A-17.4-100,200 2024	Hi-Lo-8-A-20-50,900 7075	Hi-Lo-8-A-17.4-100,200 2024	Lo-Hi-Lo-8-A-20-10,200 7075	Lo-Hi-Lo-8-A-17.4-10,200 2024	Hi-Lo-Hi-8-A-20-50,900 7075	Hi-Lo-Hi-8-A-17.4-100,200 2024	Random-8-A-20-10,200 7075	Random-8-A-20-50,900 7075	Random-8-A-17.4-50,100 2024	Random-8-A-17.4-100,200 2024	Random-8-A-0-30,000 7075	Random-8-A-0-50,000 2024	Random-8-A-0-100,000 2024
Lo-Hi-8-A-20-10,200	7075			Yes													
Lo-Hi-8-A-20-50,900	7075			Yes													
Lo-Hi-8-A-17.4-100,200	2024	2.83	2.78														
Hi-Lo-8-A-20-50,900	7075					Yes											
Hi-Lo-8-A-17.4-100,200	2024				1.69												
Lo-Hi-Lo-8-A-20-10,200	7075							Yes									
Lo-Hi-Lo-8-A-17.4-10,200	2024						1.72										
Hi-Lo-Hi-8-A-20-50,900	7075									Yes							
Hi-Lo-Hi-8-A-17.4-100,200	2024								2.35								
Random-8-A-20-10,200	7075												No	Yes			
Random-8-A-20-50,900	7075												No	Yes			
Random-8-A-17.4-50,100	2024										1.19	1.09					
Random-8-A-17.4-100,200	2024										2.03	1.85					
Random-8-A-0-30,000	7075															No	Yes
Random-8-A-0-50,000	2024														1.47		
Random-8-A-0-100,000	2024														2.35		

Yes — Sample geometric means are significantly different

1.78 — Ratio of sample geometric means, $\frac{\text{Top group}}{\text{Side group}}$

TABLE VIII.- RESULTS OF STATISTICAL ANALYSIS OF VARIABLE-AMPLITUDE FATIGUE TESTS ON 2024-T3 AND 7075-T6 ALUMINUM-ALLOY SPECIMENS - Concluded

(d) Effect of number of cycles per block

Side group \ Top group	2024-18-B-17.4-Lo-Hi 100,000	2024-18-B-17.4-Lo-Hi 500,000	2024-18-B-17.4-Hi-Lo 100,000	2024-18-B-17.4-Hi-Lo 500,000	2024-8-A-17.4-Random 50,100	2024-8-A-17.4-Random 100,200	2024-8-A-0-Random 50,000	2024-8-A-0-Random 100,000	7075-8-A-20-Lo-Hi 10,200	7075-8-A-20-Lo-Hi 50,900	7075-8-A-20-Random 10,200	7075-8-A-20-Random 50,900
2024-18-B-17.4-Lo-Hi 100,000		Yes										
2024-18-B-17.4-Lo-Hi 500,000	2.2											
2024-18-B-17.4-Hi-Lo 100,000				No								
2024-18-B-17.4-Hi-Lo 500,000			0.79									
2024-8-A-17.4-Random 50,100						Yes						
2024-8-A-17.4-Random 100,200					1.70							
2024-8-A-0-Random 50,000								Yes				
2024-8-A-0-Random 100,000							1.60					
7075-8-A-20-Lo-Hi 10,200										No		
7075-8-A-20-Lo-Hi 50,900									1.0			
7075-8-A-20-Random 10,200												No
7075-8-A-20-Random 50,900											1.10	

(e) Effect of stress step

Side group \ Top group	2024-17.4-A-Random-50,100 8	2024-17.4-A-Random-100,200 8	2024-17.4-A-Random-100,000 18
2024-17.4-A-Random-50,100 8			Yes
2024-17.4-A-Random-100,200 8			No
2024-17.4-A-Random-100,000 18	1.49	0.88	

(f) Effect of gust frequency curve

Side group \ Top group	2024-18-17.4-Random-100,000 A	2024-18-17.4-Random-500,000 B
2024-18-17.4-Random-100,000 A		No
2024-18-17.4-Random-500,000 B	1.36	

	Yes
1.78	

Yes — Sample geometric means are significantly different

1.78 — Ratio of sample geometric means, $\frac{\text{Top group}}{\text{Side group}}$

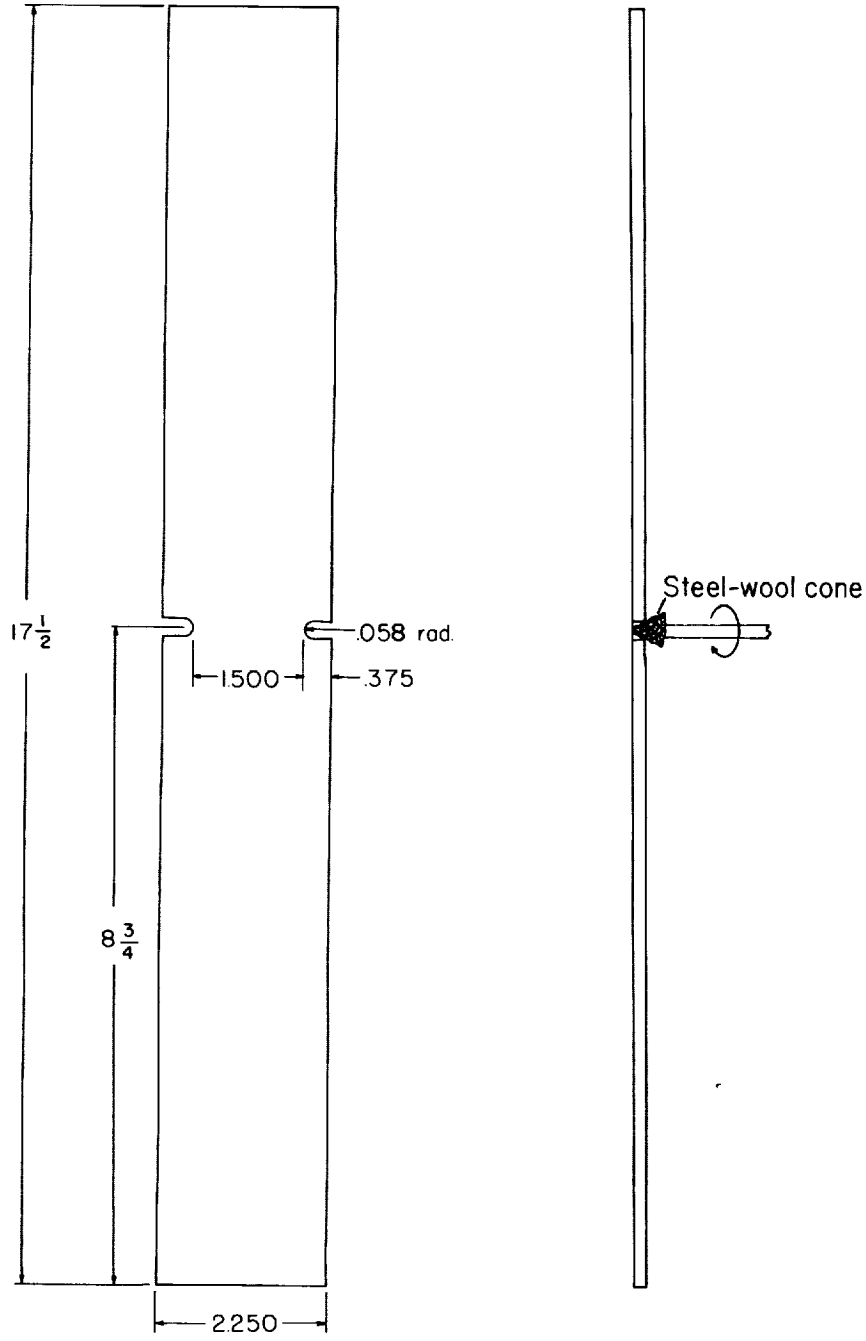

(a) Specimen dimensions. (b) Deburring technique.

Figure 1.- Sheet-specimen details.

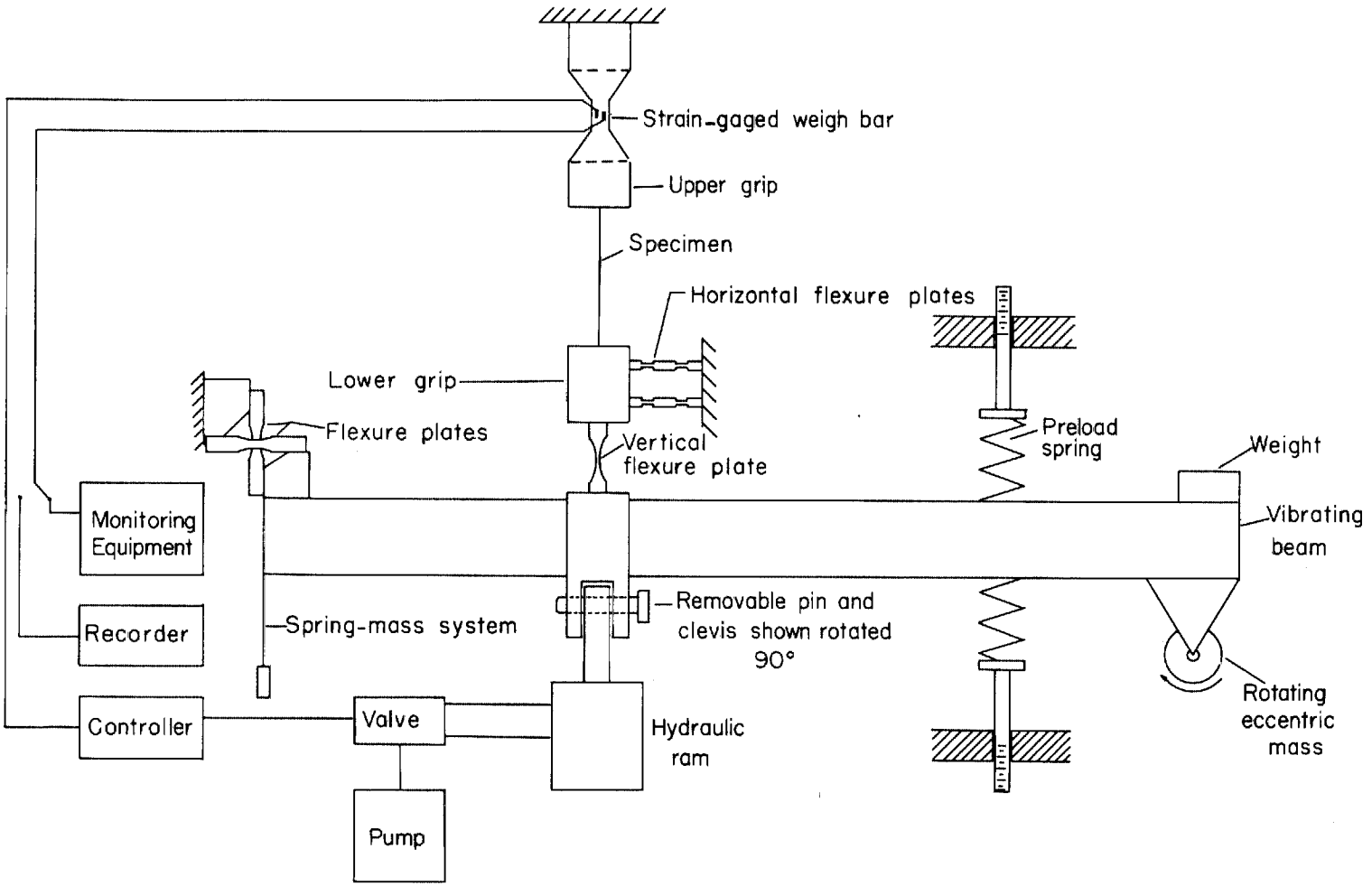

Figure 2.- Schematic diagram of fatigue testing machine.

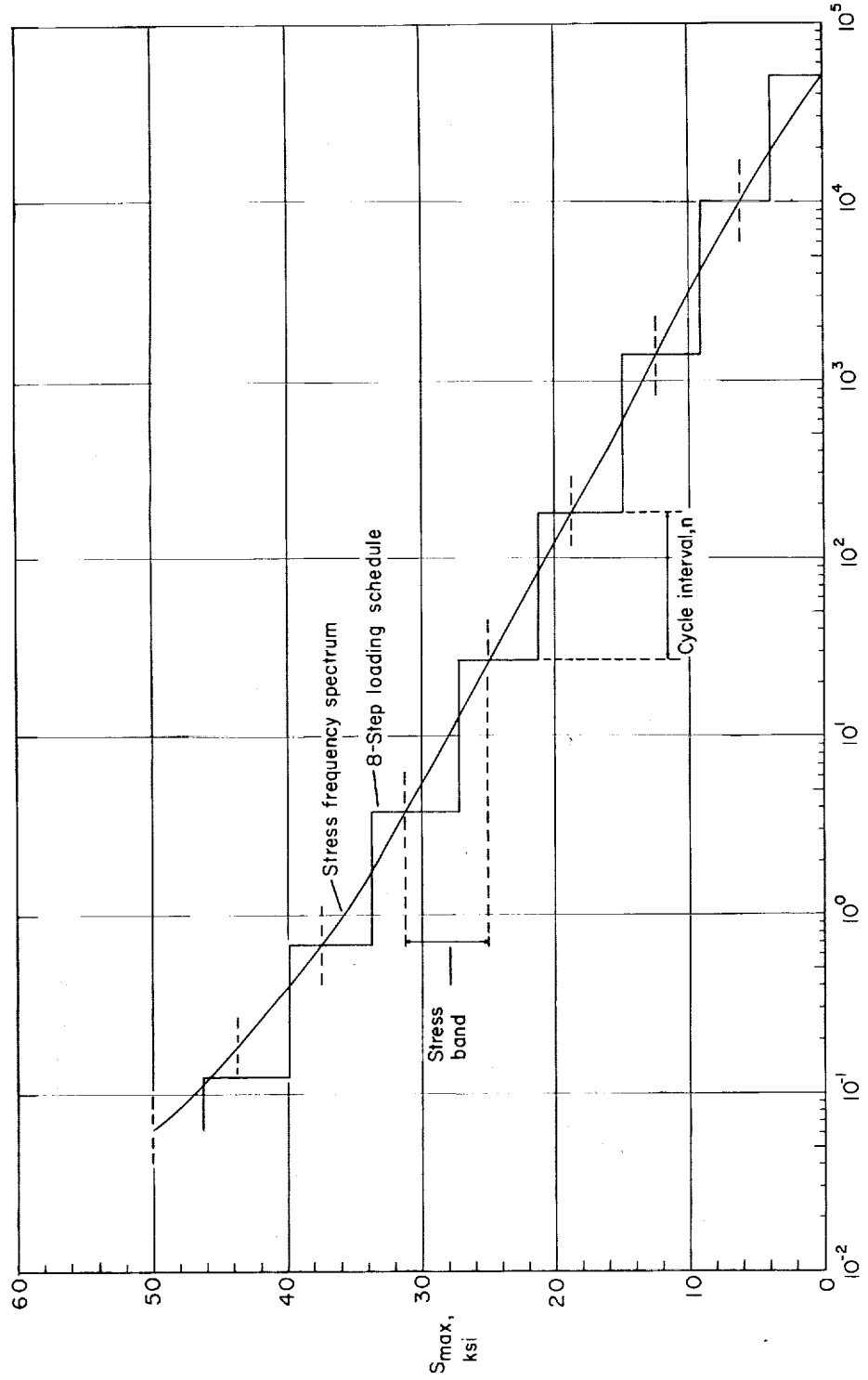

Figure 3.- Eight-step approximation of stress frequency spectrum.

L-798

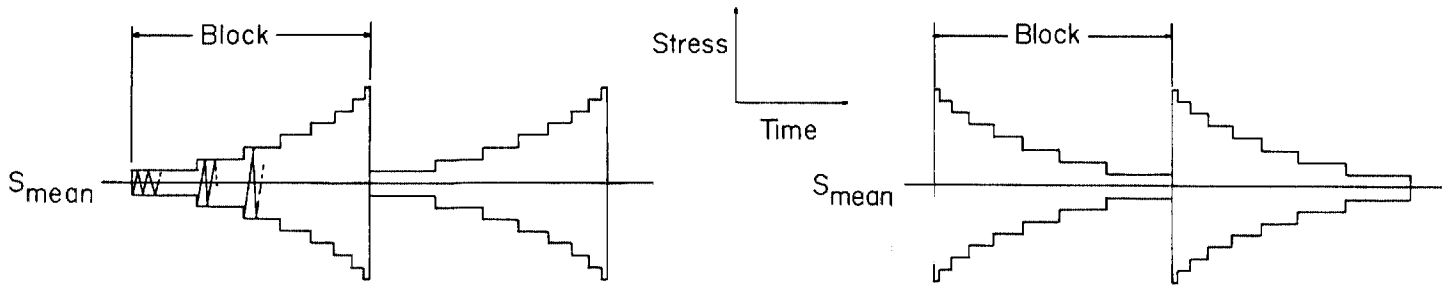

(a) Lo-Hi sequence.

(b) Hi-Lo sequence.

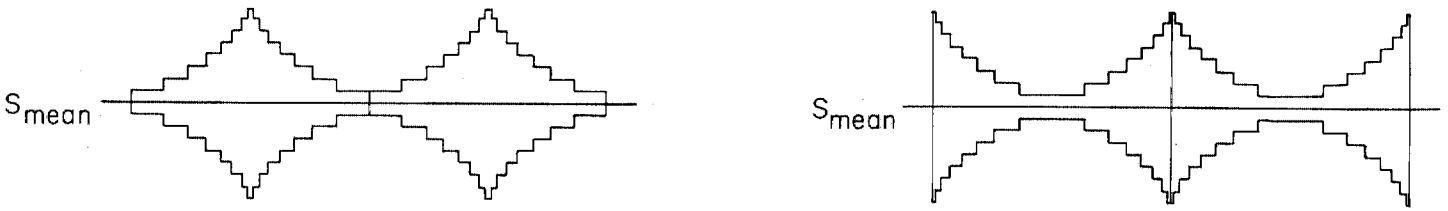

(c) Lo-Hi-Lo sequence.

(d) Hi-Lo-Hi sequence.

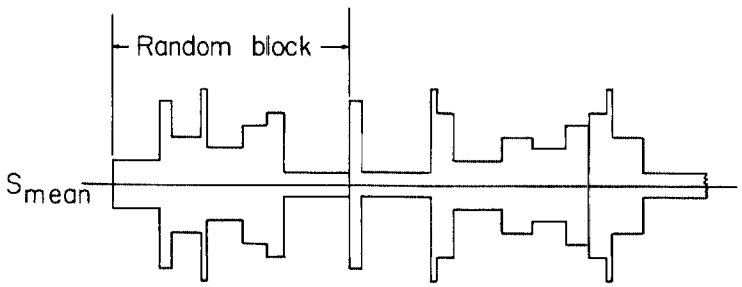

(e) Random sequence.

Figure 4.- Schematic diagrams of loading sequence.

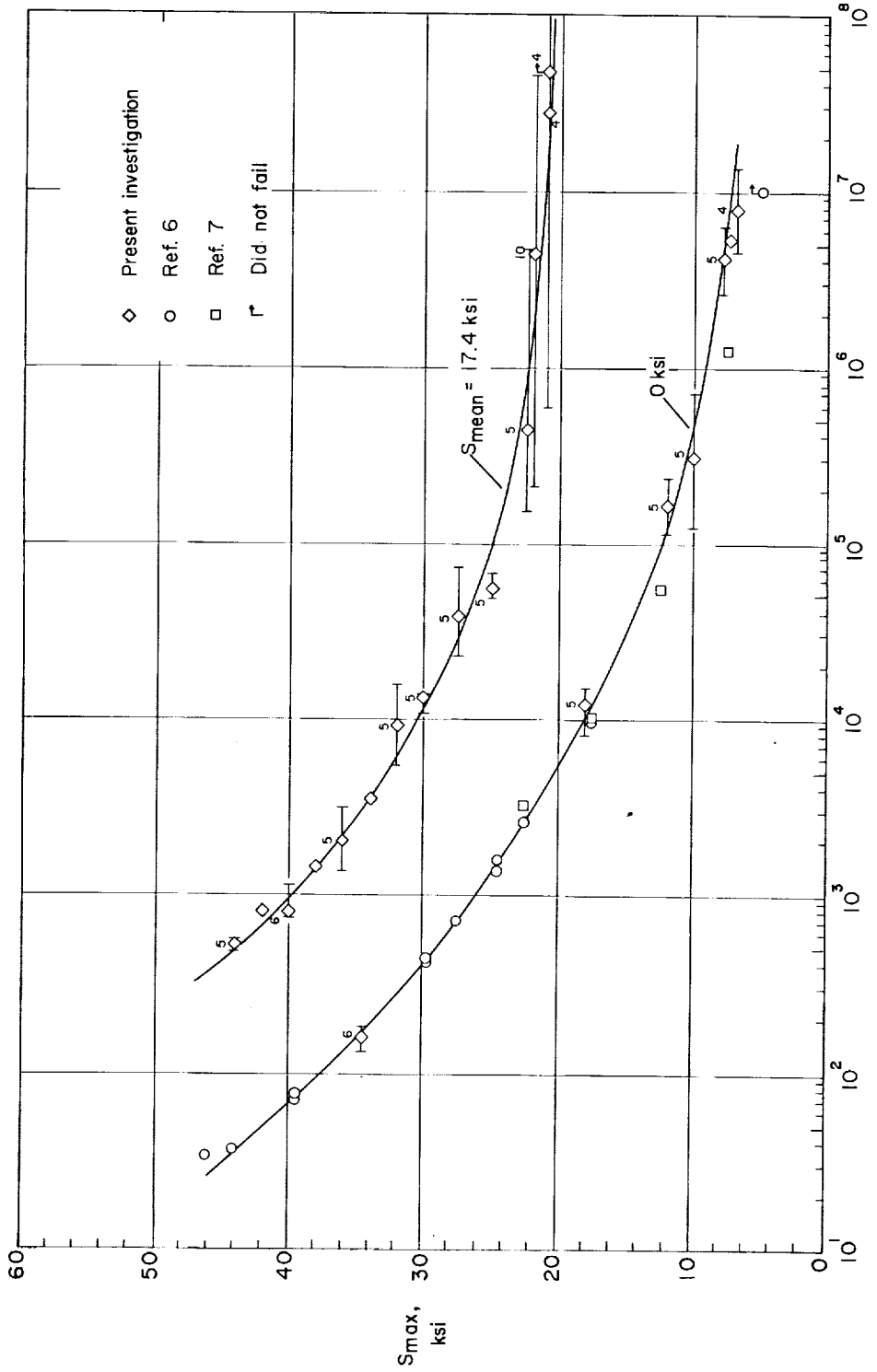

Figure 5.- Results of constant-amplitude fatigue tests of 2024-T3 aluminum-alloy specimens. (Ticks represent scatter bands and numerals indicate number of tests in each group.)

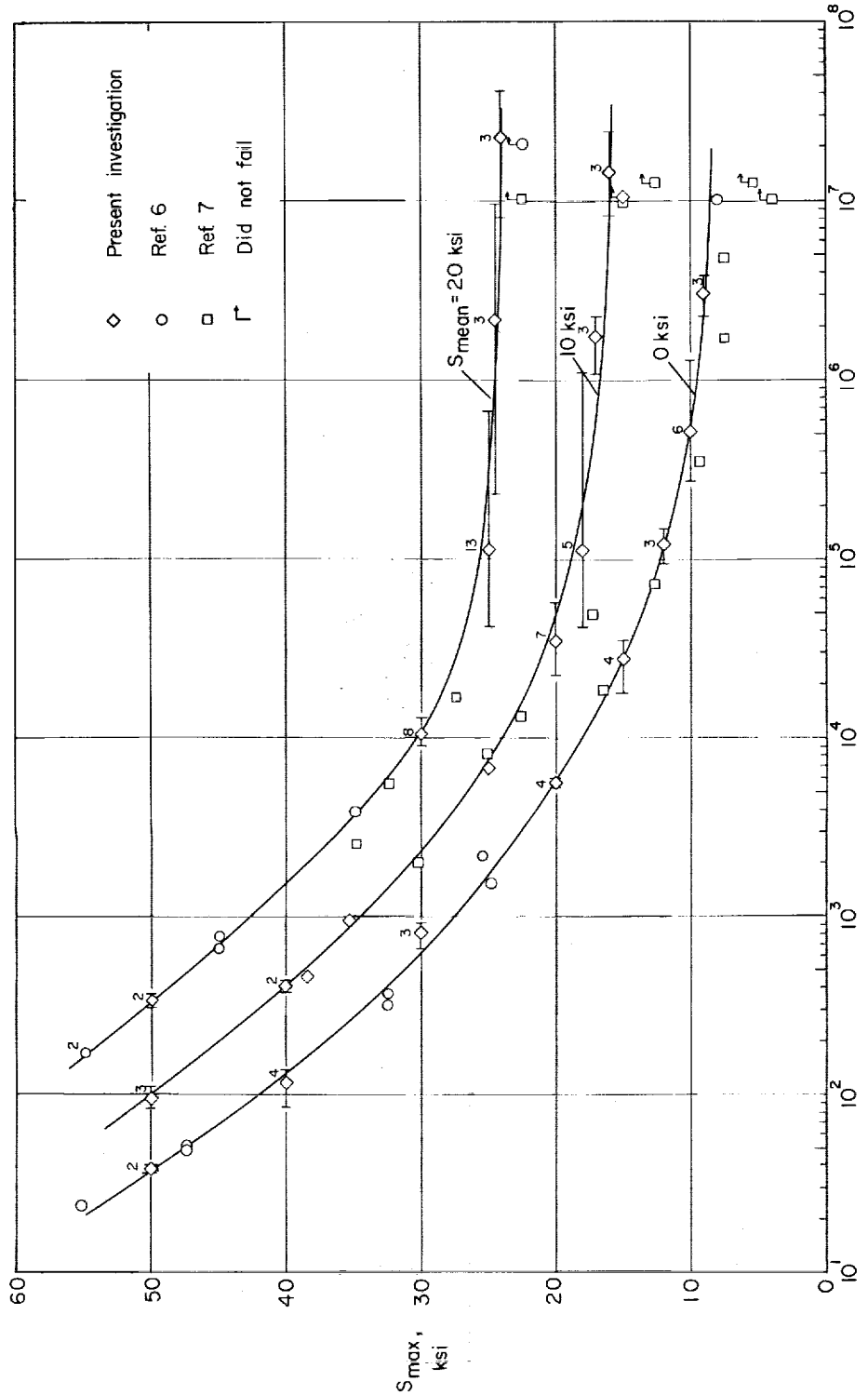

Figure 6.- Results of constant-amplitude fatigue tests of 7075-T6 aluminum-alloy specimens. (Ticks represent scatter bands and numerals indicate number of tests in each group.)

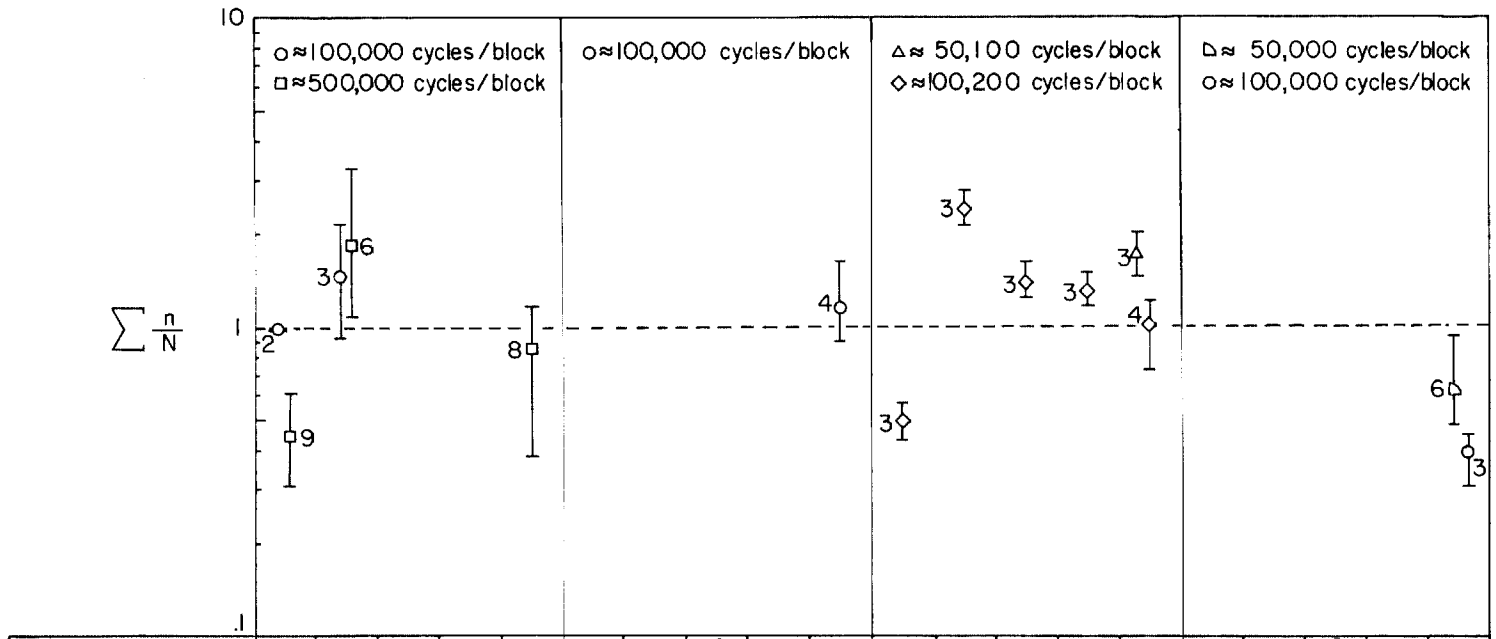

Sequence	Lo-Hi	Hi-Lo	Lo-Hi-Lo	Hi-Lo-Hi	Random	Lo-Hi	Hi-Lo	Lo-Hi-Lo	Hi-Lo-Hi	Random	Lo-Hi	Hi-Lo	Lo-Hi-Lo	Hi-Lo-Hi	Random	Lo-Hi	Hi-Lo	Lo-Hi-Lo	Hi-Lo-Hi	Random
S_{mean}, ksi	17.4					17.4					17.4					0				
Stress steps	18					18					8					8				
Gust frequency curve	B					A					A					A				

Figure 7.- Results of variable-amplitude fatigue tests of 2024-T3 aluminum-alloy specimens. (Ticks represent scatter bands and numerals indicate number of tests in each group.)

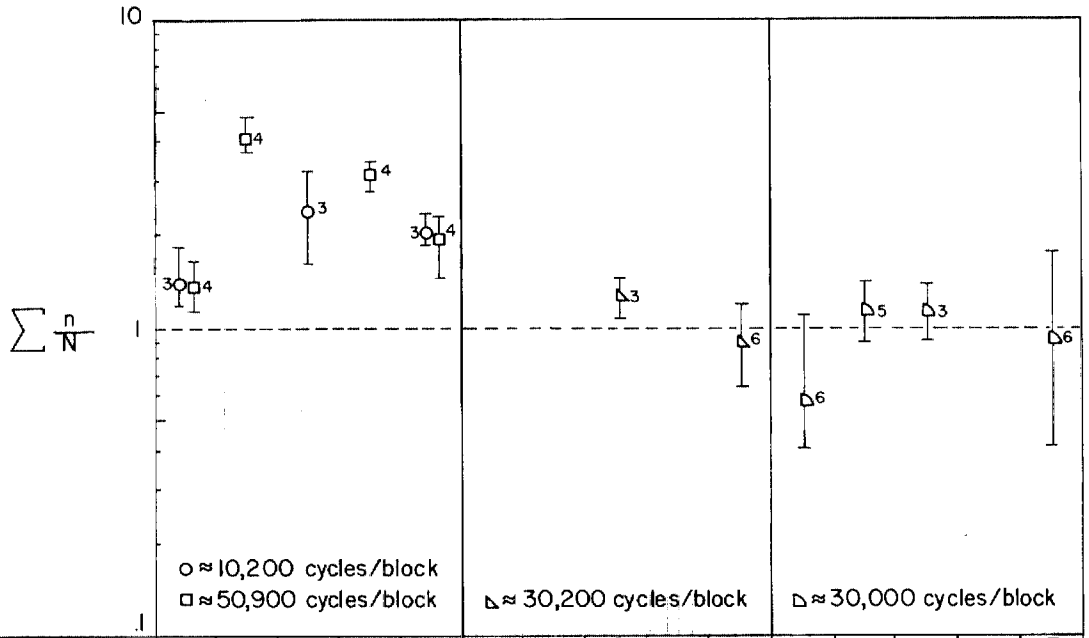

Sequence	Lo-Hi	Hi-Lo	Lo-Hi-Lo	Hi-Lo-Hi	Random	Lo-Hi	Hi-Lo	Lo-Hi-Lo	Hi-Lo-Hi	Random	Lo-Hi	Hi-Lo	Lo-Hi-Lo	Hi-Lo-Hi	Random
S_{mean}, ksi	20					10					0				
Stress steps	8					8					8				
Gust frequency curve	A					A					A				

Figure 8.- Results of variable-amplitude fatigue tests of 7075-T6 aluminum-alloy specimens. (Ticks represent scatter bands and numerals indicate number of tests in each group.)

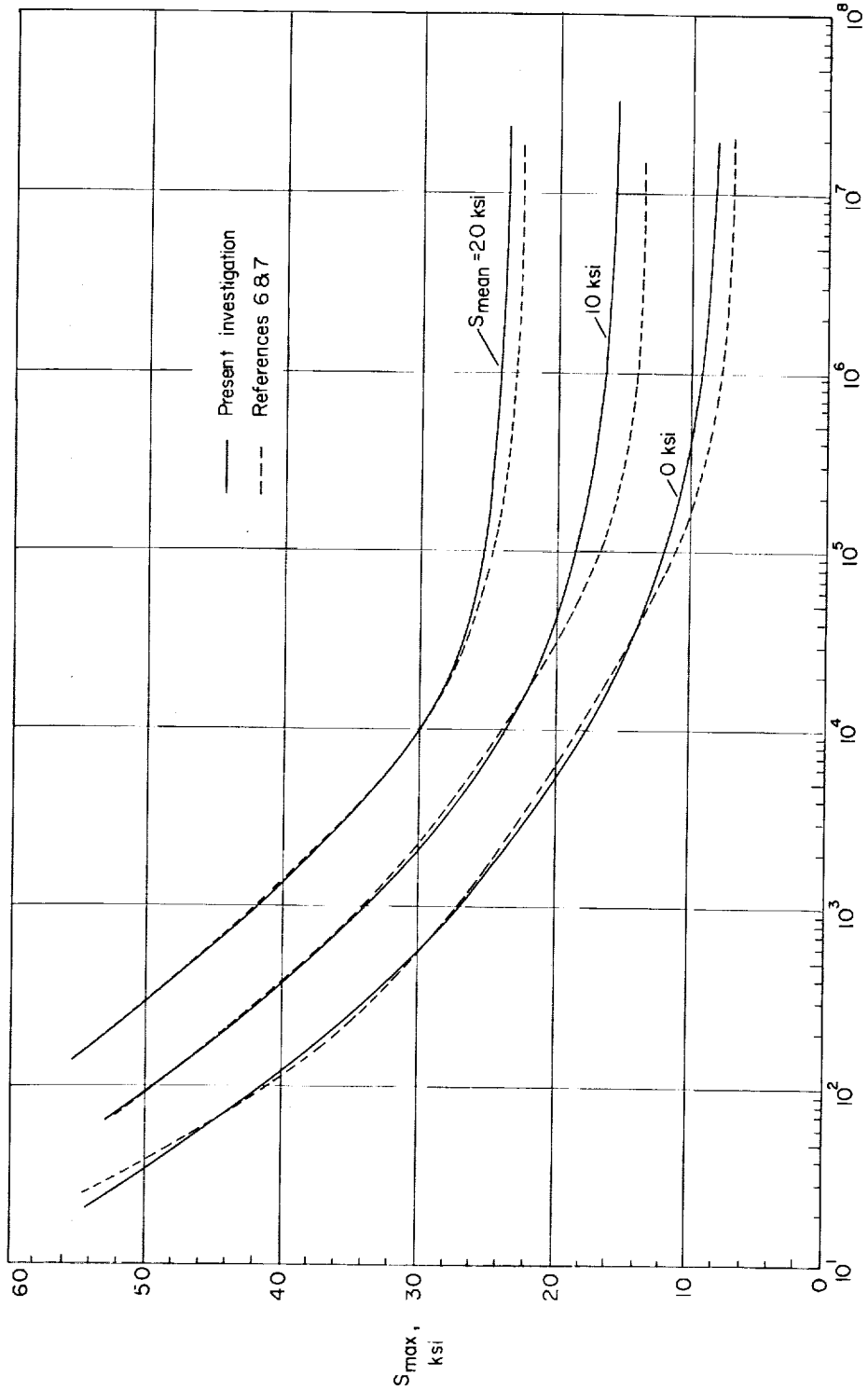

Figure 9.- S-N curves for 7075-T6 aluminum-alloy specimens with K_T = 4.0.

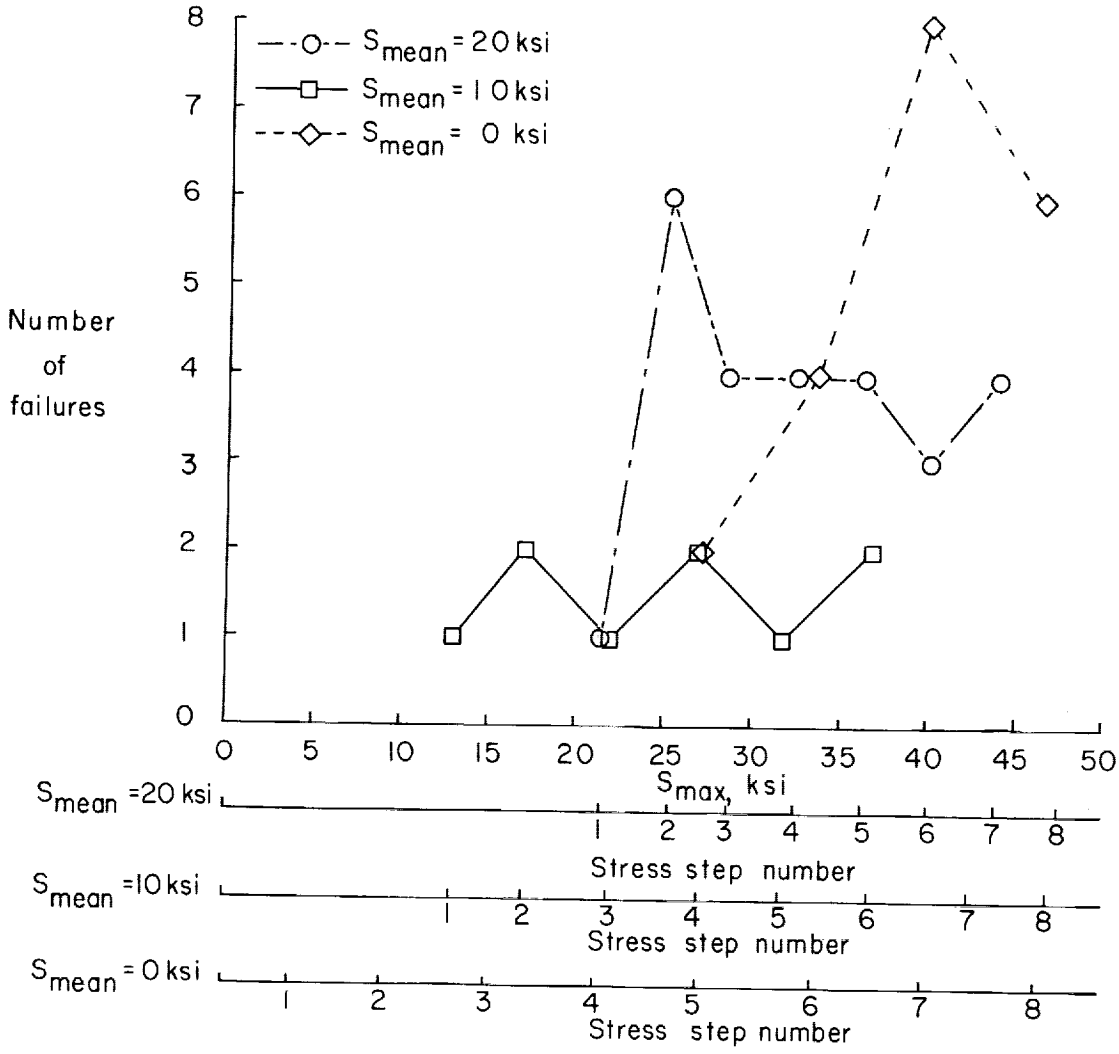

Figure 10.- Stress at failure in variable-amplitude fatigue tests of 7075-T6 aluminum-alloy specimens.